Polymer 49 (2008) 4427–4432

Contents lists available at ScienceDirect

Polymer

journal homepage: www.elsevier.com/locate/polymer

Glass transition behavior and dynamic fragility in polylactides containing mobile and rigid amorphous fractions

Ester Zuza, Jone M. Ugartemendia, Alberto Lopez, Emilio Meaurio, Ainhoa Lejardi, Jose-Ramon Sarasua*

University of the Basque Country (EHU-UPV), School of Engineering, Alameda de Urquijo s/n, 48013 Bilbao, Spain

ARTICLE INFO

Article history:
Received 25 March 2008
Received in revised form 6 August 2008
Accepted 8 August 2008
Available online 13 August 2008

Keywords:
Poly(L-lactide)
Poly(D,L-lactide)
Crystalline confinement

ABSTRACT

The segmental dynamics of polylactide chains covering the $T_g - 30\,^{\circ}C$ to $T_g + 30\,^{\circ}C$ range was studied in absence and presence of a crystalline phase by dynamic mechanical analysis (DMA) using the framework provided by the WLF theory and the Angell's dynamic fragility concept. An appropriate selection of stereoisomers combined with a thermal conditioning strategy to promote crystallization (above T_g) or relaxation of chains (below T_g) was revealed as an efficient method to tune the ratio of the rigid and mobile amorphous phases in polylactides. A single bulklike mobile amorphous phase was taken for poly(D,L-lactide) (PDLLA). In turn three phases, comprising a mobile amorphous fraction (MAF, X_{MA}), a rigid amorphous fraction (RAF, X_{RA}) and a crystalline fraction (X_c) were determined in poly(L-lactide) (PLLA) by modulated differential scanning calorimetry (MDSC) according to a three-phase model. The analysis of results confirms that crystallinity and RAF not only elevate the T_g and the breadth of the glass transition region but also yields an increase in dynamic fragility parameter (m) which entails the existence of a smaller length-scale of cooperativity of polylactide chains in confined environments. Consequently it is proposed that crystallinity is acting in polymeric systems as a topological constraint that, preventing longer range dynamics, provides a faster segmental dynamics by the temperature dependence of relaxation times according to the strong–fragile scheme.

1. Introduction

Although in many aspects there is still a lack of understanding of the fundamentals that govern the segmental relaxation of macromolecules in both non-confined and confined environments, it is well established that constraints on polymer chains, caused for instance by crosslinking or crystallinity, affect the T_g behavior. In thermosetting systems it is confirmed that T_g shifts to higher temperatures as crosslink density increases, since chains find a growing hindrance to relax [1].

Concerning semicrystalline polymers, macromolecules are longer than the thickness of the crystal lamellae, thus they can cross the phase boundaries and cause various degrees of coupling; on weak coupling, the dynamics of the non-crystalline segments shows usually a broadening of the glass transition region, yet on stronger coupling the non-crystalline material may also show a distinct glass transition, at a higher temperature of the bulk amorphous phase due to a rigid amorphous phase [2]. Restricted dynamics due to crystalline confinement and the presence of a rigid amorphous phase have been reported for example in poly(phenylene sulphide) (PPS) [3,4], poly(ether ether ketone) (PEEK) [5], syndiotactic polystyrene [6] or polycarbonate [7]. Concerning poly(L-lactide) [8], when prepared with intermediate degree of crystallinity, two T_g dynamics were observed; the high T_g dynamics was attributed to the hindered motions of the amorphous phase within the lamellar stacks.

The occurrence of the glass transition in polymers is associated to cooperative motions of macromolecular chain segments. Cooperative segment length (ξ) results to be in the range of 1–3 nm at the glass transition temperature depending on the glass-forming polymer [9]. Often found in the literature is the not unambiguous query as to whether the chain mobility is increased or decreased by constraints. The fact that the T_g appears at higher temperatures in crosslinked, semicrystalline and fiber reinforced polymer systems has usually been interpreted as a restricted dynamics of polymer chains in confined environments. Moreover, the fact that the T_g in confined environments may be suppressed [10,11] supports the idea that cooperativity of chain motion is impeded when the dimension of the topological constraint (d) is smaller than ξ.

However, controversial results are reported for confined and unconfined conditions of polymer chains when describing the segmental dynamics by the temperature dependence of relaxation times according to the strong–fragile scheme. The glass transition of supercooled polymer liquids is a kinetic process in which the relaxation time of the constituent molecules can increase by many orders

* Corresponding author.
E-mail address: jr.sarasua@ehu.es (J.-R. Sarasua).

0032-3861/$ – see front matter © 2008 Elsevier Ltd. All rights reserved.
doi:10.1016/j.polymer.2008.08.012

of magnitude in a narrow temperature range. The glassy state is unstable because a glass is continually relaxing towards equilibrium and therefore the different related properties are also changing. The dynamic fragility [12] accounts for the ease with which the glass transition is completed. According to Angell [13], a polymer is defined dynamically fragile when there is little impediment for segmental relaxation of chains, carrying rapidly a drastic change in properties (viscosity, modulus, etc.) at the T_g. During the last years the fragility dilemma of liquids has raised research interests and particular efforts have been carried out to systematize the different polymers according to the fragility parameter [13,18].

Early studies on polymer glasses using the coupling scheme [19] revealed a relaxation process delayed by chain length due to entanglements. However, when studying the segmental dynamics in model polymer networks, the description of the temperature dependence of relaxation times according to the strong–fragile scheme showed an increase in dynamic fragility with crosslinking density [1]. Similar increased fragilities were found by molecular modeling studies simulating the relaxation behavior of polystyrene chains in confined conditions such as those found inside the galleries of silicate layers in nanocomposites [10].

In this work we have focused on crystalline confinement and its effect on T_g and dynamic fragility of polylactides. There is a considerable interest in understanding the temperature dependence of segmental relaxation of polymer chains in presence of a crystalline phase. Early attempts were made with semicrystalline polymers [20] such as poly(ethylene terephthalate), polypropylene or poly(dimethylsiloxane) but the authors pointed that the interpretation of neither the relaxation function nor coupling parameters was straightforward. Studies on polymers with high T_m such as PEEK [21] and PPS [22] report that the presence of crystals slows down the relaxation of chains. However, in more flexible chains, for example in PVDF or some blends, the relaxation time is reported to be unaffected or even to decrease with crystalline confinement [23,24]. Recently, PLLA has been the subject of several segmental dynamics studies [25–29]. An unchanging dynamic fragility, the T_g-normalized temperature dependence of a property, was obtained during crystallization of PLLA suggesting that the segmental dynamics is not sensitive to the different degree of crystallinity [25]; yet the molecular dynamics of bulklike mobile chains in PDLLA was not conducted in this work. Finally, a significant reduction in T_g has been reported for PLLA crystallized under partially constrained conditions [29] which was attributed to an increment of net free volume in the amorphous phase when the polymer was prevented from shrinking during crystallization.

The above apparently contradictory results justify our study on T_g and dynamic fragility. We have chosen polylactide as model polymer since, selecting the enantiomer composition and a proper thermal conditioning during processing, crystalline and rigid amorphous fractions could be tuned. DMA provides changes of selected properties with frequency for a range of temperatures around the glass transition [30], hence this method was used to determine the dynamic fragility of polylactide chains in presence and absence of crystalline confinement. The comparison of the dynamic fragility parameter in polylactides containing an unconfined bulk amorphous phase or a partly crystalline-confined one will allow one to draw a straightforward comparison of the differences in segmental cooperativity occurring during the relaxation processes around the T_g in both cases.

2. Experimental part

2.1. Starting materials

Poly(D,L-lactide) (PDLLA) and poly(L-lactide) (PLLA) were supplied by Purac biochem (The Netherlands). The molecular weight of both polymers was measured viscometrically in a Ubbelohde type viscometer in chloroform at 30 °C, using the relations [31]:

$$\left[\eta\right] = 2.21 \times 10^{-4} M_v^{0.77} (\mathrm{dl/g}) \quad (1)$$

$$\left[\eta\right] = 5.45 \times 10^{-4} M_v^{0.73} (\mathrm{dl/g}) \quad (2)$$

Values of $M_v = 3.8 \times 10^5$ and $M_v = 3.2 \times 10^5\ \mathrm{g\,mol^{-1}}$ were obtained, respectively, for PDLLA and PLLA.

2.2. Conformation and thermal conditioning of materials

Pellets of PDLLA and PLLA were previously dried and used as starting materials to conform 1 mm thick sheets by compression molding at 200 °C. PDLLA was solidified by water quenching. To develop a range of crystalline and rigid amorphous fractions in PLLA different cooling rates and thermal annealing strategies were used as follows. A PLLA sheet was prepared by water quenching from the melt (PLLA-WQ). Another PLLA sheet was prepared by slow cooling of the melt inside the plates of the press (PLLA-SC) until reaching the room temperature. Finally the water quenched PLLA sample was submitted to an annealing treatment in an oven at 80 °C for 3 h (PLLA-WQA).

2.3. Modulated differential scanning calorimetry

Thermal analysis was carried out on an MDSC from TA Instruments, model DSC Q200. Approximately 5–10 mg of each polymer was weighed and sealed in an aluminium pan. DSC scans were performed on sheet samples with a period of 60 s and a scan rate of 2 °C min^{-1} in a heat only process, up to 200 °C. The thermograms obtained are those of heat capacity (C_p), total heat flow (HF), reversing heat flow and non-reversing heat flow. Glass transition temperatures were measured in reversing HF curves as middle point values.

2.4. Dynamic mechanical analysis

Rectangular specimens were cut from compression molded sheets and tested on a dynamic mechanical analyzer DMA/SDT A861 from Mettler-Toledo (shear mode). Displacement and force amplitudes were properly adjusted for each sample. An isothermal conditioning strategy at a sub-T_g temperature was used to detect eventual structural changes occurring in PLLA (relaxation from RAF or aging) with respect to PDLLA. To prevent crystallization during the subsequent DMA heating scan, the PLLA-WQ samples were first homogenized in the DMA chamber at 80 °C for 2 h, quenched to 50 °C and then submitted to the selected different isothermal conditioning periods: 15, 30, 60 or 120 min. The same temperature and time conditioning were also applied to PDLLA, yet in this case no crystallization is expected and hence the homogenization step was skipped. The subsequent DMA temperature range studied was 30–90 °C, the frequency used 1 Hz, the heating rate 3 °C min^{-1}; the storage modulus (G') and the mechanical loss (tan δ) evolution with temperature were registered.

To obtain the master curves and dynamic fragility of materials new DMA measurements were conducted between 20 and 0.01 Hz in isothermal conditions from $T_g - 30$ °C to $T_g + 30$ °C every 3 °C. Master curves for the storage modulus G' and tan δ were composed by shifting the values obtained in isothermal conditions along the frequency scale according to the time–temperature principle. The time–temperature superposition principle was used taking into

account that it is only valid if the width at half-maximum of the relaxation process does not change with temperature [32].

3. Results and discussion

3.1. RAF, MAF and crystalline fractions as determined by MDSC

Fig. 1 shows the heat capacity MDSC curves of PDLLA and PLLA on heating. Please note that three different thermal conditioning strategies were followed to tune the crystalline fraction of PLLA as mentioned in the experimental part; in addition, as it will be shown below, crystallization of the sample entailed the development of a rigid amorphous fraction. PDLLA shows a single transition corresponding to the T_g at 50 °C with a heat capacity change at T_g of 0.628 J g^{-1} °C^{-1}, a value that agrees reasonably well with those reported for fully amorphous polylactides [33]. The T_g of PLLA-WQ is 51 °C, very close to that of PDLLA, reflecting a nearly amorphous material after water quenching; hence during the MDSC in this case a cold crystallization peak around 90 °C can also be observed and, finally, the crystal melts around 170 °C.

It is noted that melting in all PLLAs of Fig. 1 is accompanied by a small exothermal event. This exothermal signal overlapping the melting peak has been already reported elsewhere and has been attributed to a recrystallization of already existing α crystals into an α polymorph of higher perfection [34]. Looking at the two bottom curves corresponding to the annealed and slowly cooled crystallized PLLA samples, a suppression of cold crystallization behavior and a broadening of the glass transition are observed, as expected, taking into account that these treatments were specifically chosen to develop crystallinity in PLLA. Finally, a remarkable shift in T_g is also noted in crystalline PLLAs, larger in 15–21 °C compared to the T_g found in fully amorphous PDLLA or in nearly amorphous PLLA-WQ.

The crystallization and melting signals superimposed in the total heat flow of PLLAs could be separated in the reversing HF and non-reversing HF signals by MDSC. Fig. 2 shows the results obtained with PLLA that were used in as received pellet form. As can be observed the total HF decomposes in an endothermal HF signal due to melting (appearing in the non-reversing HF curve) and in an exothermal HF signal (appearing in the reversing HF curve). Hence using MDSC allows one to separate the crystallization process hidden during crystal melting by standard DSC. Since MDSC also provides the means to obtain direct measurement of *Cp* vs. temperature [35], we could determine the crystalline, RAF and MAF by using the three-phase model described below.

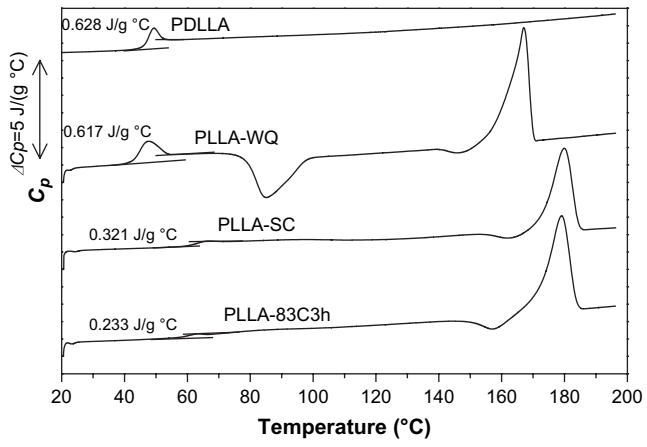

Fig. 1. Specific heat (C_p) curves and specific heat change at T_g (ΔC_p) measures of polylactides having different crystalline, RAF and MAF (see Table 1). PDLLA: quenched in water from the melt, not annealed; PLLA-WQ: quenched in water from the melt, not annealed; PLLA-WQA: quenched in water from the melt and annealed at 80 °C for 3 h; PLLA-SC: slowly cooled from the melt inside the mould.

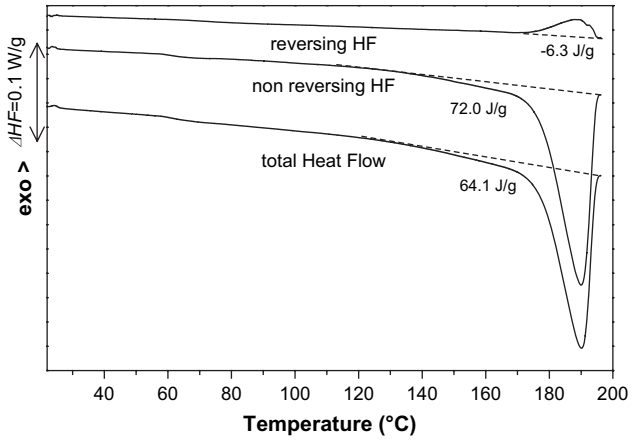

Fig. 2. MDSC heat flow curves of PLLA analyzed in as-received pellet form.

Table 1
Thermal properties of polylactides by MDSC

	T_g (°C)	ΔC_p (J g^{-1} °C^{-1})	$\Delta C_p/\Delta C_p^0$	ΔH_{c1} (J g^{-1})	ΔH_{c2} (J g^{-1})	ΔH_m (J g^{-1})	χ_c	χ_{RA}	χ_{MA}
PDLLA	50	0.623	1	–	–	–	0	0	1
PLLA-WQ	51	0.617	0.990	30	17.2	48.1	0.008	0.002	0.990
PLLA-SC	71	0.321	0.515	0	6.0	41.4	0.334	0.151	0.515
PLLA-WQA	65	0.233	0.374	0	7.9	50.9	0.406	0.220	0.374

ΔC_p: specific heat change at T_g; ΔC_p^0: specific heat change at T_g in fully amorphous polylactide; ΔH_{c1}: exothermal enthalpy change (cold crystallization peak); ΔH_{c2}: exothermal enthalpy change (just before melting), ΔH_m: melting enthalpy.

Table 1 shows the values of the thermal properties of PDLLA and PLLA obtained by MDSC to determine, according to a three-phase model, the fractions of the existing possible phases, the crystalline (χ_c), the mobile amorphous (χ_{MA}) and the rigid amorphous (χ_{RA}) phases. Table 1 reports the T_g position, the specific heat change at T_g (ΔC_p), the heats of cold crystallization (ΔH_{c1}) and crystallization just before melting (ΔH_{c2}), and the melting enthalpy of polylactides.

Crystalline index of PLLA was determined according to Eq. (3). The standard enthalpy values of fully crystalline polylactide polymorphs used in the literature are not always coincident. Although many crystalline index calculations for α-polylactides appearing in the literature have been made with the value of $\Delta H_m{}^0 = 93$ J g^{-1} [36], a better correlation between WAXS and DSC was obtained using $\Delta H_m^0 = 106$ J g^{-1} [37,38].Thus the later value was used in our calculations of crystalline fraction in PLLAs.

Accepting that there is a single bulk mobile amorphous phase in PDLLA, the bulklike MAF in PLLA can be determined with Eq. (4) as the ratio of the specific heat change at T_g of PLLA (ΔC_p) and PDLLA (ΔC_p^0), both obtained experimentally by MDSC. Finally, according to a three phase model the RAF can be determined by Eq. (5).

$$\chi_c = \frac{\Delta H_m - (\Delta H_{c1} + \Delta H_{c2})}{\Delta H_m^0} \quad (3)$$

$$\chi_{MA} = \frac{\Delta C_p}{\Delta C_p^0} \quad (4)$$

$$\chi_{RA} = 1 - \chi_c - \chi_{MA} \quad (5)$$

The results obtained for the fractions of crystalline (χ_c), mobile amorphous (χ_{MA}) and rigid amorphous (χ_{RA}) phases of PDLLA and PLLA samples can also be read in Table 1. Assuming that PDLLA contains a single MAF, it is observed that PLLAs contain both MAF

and RAF. It is remarkable that, when quenched in water (PLLA-WQ), PLLA gives an inconsiderable crystalline and RAF and therefore it is nearly amorphous. However, annealing of the quenched PLLA at a temperature above T_g (PLLA-WQA) or non-isothermal crystallization from the melt results in crystalline development. Finally, following with the crystalline PLLAs, it is observed that crystalline development carries with it a rigid amorphous fraction, since larger values of χ_{RA} correspond to larger χ_c values.

3.2. RAF and MAF as determined by DMA

Fig. 3 shows the DMA curves for storage modulus and tan δ of PDLLA. A single dissipation peak corresponding to the T_g in PDLLA appears for all isothermal conditioning times unchanged and centered at 60 °C. It is also noted that the T_g transition of PDLLA is in all cases quite narrow starting at approx. 50 °C and ending at 70 °C. It can be confirmed from these results that the isothermal conditioning time used at 50 °C had no significant effect in glass transition behavior of PDLLA.

Fig. 4 shows the DMA curves for storage modulus and tan δ of PLLA. It is noted in this case that the T_g transition of PLLA is broader, starting at approx. 50 °C and finishing at 90 °C. Moreover tan δ shows a double peak behavior and is affected by the isothermal conditioning time at 50 °C. PLLA after crystallization at 80 °C without thermal conditioning or with a small period of 15 min at 50 °C shows a prominent T_g peak centered at 75 °C and a small peak at 60 °C that increases in height as isothermal conditioning time increases. The

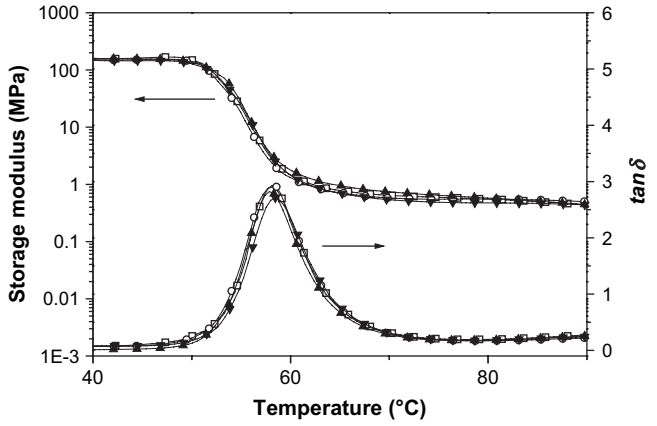

Fig. 3. Dynamic mechanical curves of PDLLA isothermally conditioned at 50 °C for different times: □ 15 min, ○ 30 min, ▲ 60 min, ▼ 120 min. Frequency: 1 Hz.

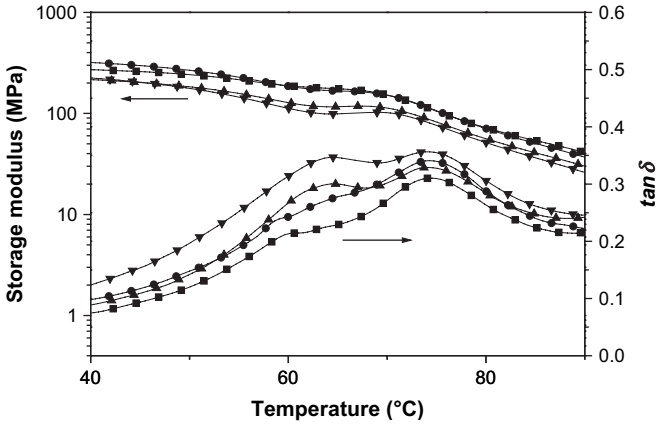

Fig. 4. Dynamic mechanical curves of PLLA-WQA isothermally conditioned at 50 °C for different times: □ 15 min, ○ 30 min, ▲ 60 min, ▼ 120 min. Frequency: 1 Hz.

lower T_g peak in semicrystalline PLLA is coincident with the T_g peak position of PDLLA and suggests the presence in PLLA of a mobile fraction that coexists with a larger amount of RAF which is giving the T_g peak centered at 75 °C. The fact that the relative heights of T_g dissipation peaks in PLLA vary with isothermal conditioning time entails that some chains initially in RAF are converting into MAF due to a time dependent relaxation process proceeding at 50 °C.

In order to determine the rigid and mobile amorphous fractions in PLLA by DMA the percent area of peak 1 (attributed to MAF) over the total area in tan δ was calculated. Loss factor curves obtained in DMA were fit to gaussian profiles using Kaleidagraph. Because the loss factor peaks corresponding to the glass transition of the rigid and mobile amorphous phases are poorly resolved from surrounding contributions, only the experimental data between 58 and 80 °C were included for the fittings. To further reduce fitting artifacts, both peaks were fit assuming identical width. These simplifications can introduce errors in the absolute areas of the peaks, but are necessary to obtain comparable results free of senseless fitting artifacts. In addition the sensitivity of both relaxation peaks is assumed identical. The quantitative analysis provided the following MAF values for $t = 15$ min, $t = 30$ min, $t = 60$ min and $t = 120$ min conditioned PLLA-WQA respectively: $\chi_{MA} = 0.39$, $\chi_{MA} = 0.41$, $\chi_{MA} = 0.46$ and $\chi_{MA} = 0.48$. Hence the quantitative determination by DMA proves that the rigid amorphous phase of PLA is partly converting into a mobile amorphous phase by a thermal conditioning treatment at a sub-T_g temperature.

Since there is no significant sign of change either in the position or in the height of the loss tangent peak in PDLLA (Fig. 3), it should be inferred that there is no significant aging occurring at the sub-T_g temperature and thermal conditioning times selected for polylactide chains in bulklike mobile amorphous phase. Hence, the effects of thermal conditioning on T_g behavior must be interpreted in terms of relaxation of chains initially in RAF. The rigid amorphous phase has a higher T_g, hence on cooling the deviation from equilibrium values of thermodynamic parameters such as the specific volume occurs at a higher temperature [39]; this leaves a larger neat free volume excess in PLLA that explains the partial conversion of chains from RAF to MAF occurring at a sub-T_g temperature during the thermal conditioning time.

3.3. The segmental dynamics around the T_g as determined by WLF theory and Angell's dynamic fragility parameter

The dynamic fragility is related to the deviations from simple Arrhenius temperature dependence of the relaxation process. According to the Vogel–Fulcher–Tammann–Hesse (VFTH) equation the relaxation time, τ, is given in the following way [40]:

$$\tau = \tau_0 \times e^{(B/(T-T_0))}, \tag{6}$$

where τ_0, B, and T_0 are positive constants. From VFTH equation the dynamic fragility (m) is related to the steepness index in the glass transition as follows:

$$m = \left.\frac{d \log \tau}{d(T_g/T)}\right|_{T=T_g} = \frac{BT}{(T_g - T_0)^2}, \tag{7}$$

The Williams–Landel–Ferry (WLF) equation is mathematically equivalent to the VFTH equation; it is constructed to eliminate the pre-exponential factor of VFTH equation and states the temperature dependence in the following manner [41]:

$$\log \frac{\tau}{\tau_0} = \log a_T = \frac{-C_1(T - T_g)}{C_2 + T - T_g}, \tag{8}$$

C_1 and C_2 are material constants and thus the fragility parameter can be stated as follows [14]:

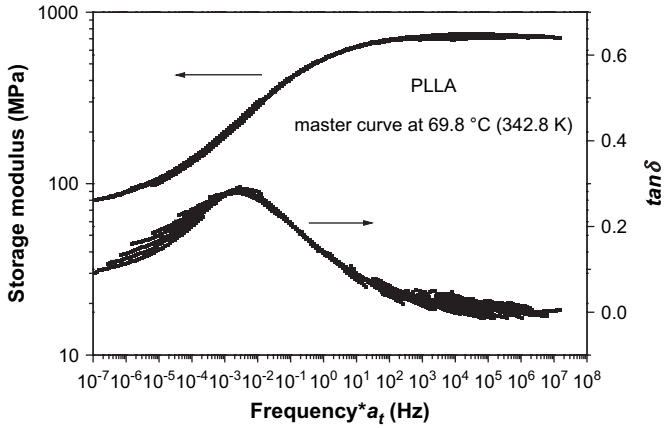

Fig. 5. Storage modulus (left) and tan δ (right) vs. frequency for PLLA-WQA, for $T = 69.8$ °C.

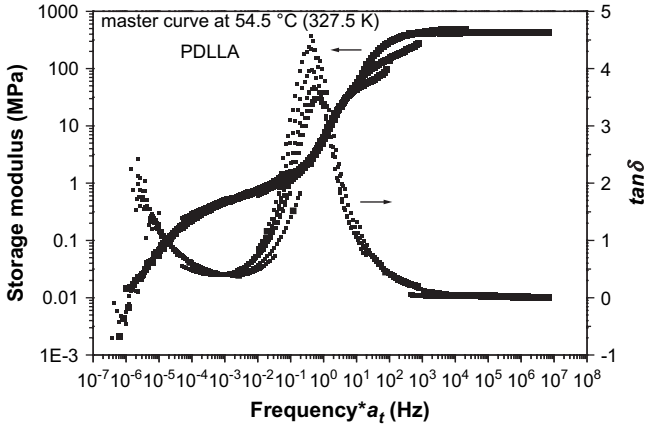

Fig. 6. Storage modulus (left) and tan δ (right) vs. frequency for PDLLA, for $T = 54.5$ °C.

Table 2
Dynamic fragility of polylactides (m) determined with Eq. (8)

	PLLA-WQA	PLLA-SC	PDLLA
Master curve T_g (K)	342.8	350.36	327.5
$m = T_g C_1/C_2$	149.9	98	69.6

PLLA-WQA: quenched in water from the melt and annealed at 80 °C for 3 h; PLLA-SC: slowly cooled from the melt inside the mould; PDLLA: quenched in water from the melt, not annealed.

$$m = \left.\frac{\mathrm{d}\,(\log a_T)}{\mathrm{d}(T_g/T)}\right|_{T=T_g} = \frac{T_g C_1}{C_2}. \quad (9)$$

The dynamic fragility parameter of polymers has been reported to fall inside an $m = 40$–200 range [17]. If m has a high value, then the material is classified as a fragile liquid, whereas when m is low it is a strong glass former. In this work we have conducted a molecular dynamics analysis by DMA in order to study the segmental relaxation of polylactide chains around the T_g in a fully amorphous medium and in the presence of a crystalline-confined environment.

In a previous work on the conformational behavior in PLLA films [42], we observed that the interphase seemed to extend over the whole interlamellar region showing the features of a semiordered metastable phase. According to the MDSC and DMA results shown above both MAF and RAF coexist in PLLA. Considering a single mobile amorphous phase in PDLLA and the presence of mobile and rigid amorphous fractions in PLLA, it seems reasonable to foresee a different molecular segmental dynamics around the T_g in both cases.

Master curves were built for PLLA and PDLLA (Fig. 5 and Fig. 6, respectively) using the DMA results obtained at different temperatures and frequencies, according to the WLF theory (Eq. (8)). C_1 and C_2 constants were deduced by fitting the shift values (a_t) experimentally obtained to the WLF equation. Finally the dynamic fragility parameter (m) was calculated with Eq. (9). The mean values for PDLLA, PLLA-SC and PLLA-WQA shown in Table 2 indicate that a larger crystalline and rigid amorphous fractions correlate with larger values of the dynamic fragility parameter (m).

Table 3 reports the calculated maximum and minimum values of fragility parameter in PLLA and PDLLA accounting for the fitting errors derived from C_1 and C_2 constants obtained during the hyperbolic representation of $(-\log a_t)$ vs. $(T - T_g)$. From these calculations resulted a dynamic fragility of PLLA falling inside the limits of $m = 130.4$ and $m = 173.0$, larger values than the dynamic fragility values obtained in PDLLA (limit values: $m = 61.1$ and $m = 79.5$). In Table 3 is also reported a broader dispersion of m in PLLA regarding PDLLA which is derived from the higher T_g value and the higher C_2 absolute error introduced in the denominator of Eq. (9).

Angell's plot in which log a_t is represented in ordinates vs. T_g/T in abscissa is also a good method to compare the segmental dynamics of different glass forming polymer liquids. Fig. 7 shows these plots for PDLLA and PLLA. As can be observed PDLLA shows a near

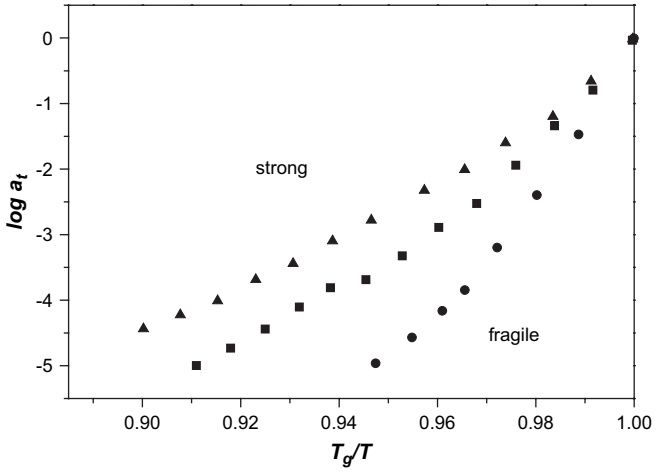

Fig. 7. Angell's plot, log a_t vs. T_g/T: PDLLA (▲), PLLA-SC (■) and PLLA-WQA (●). PLLA-WQA: quenched in water from the melt and annealed at 80 °C for 3 h; PLLA-SC: slowly cooled from the melt inside the mould.

Table 3
Minimum and maximum values (m_{min} and m_{max}) of the dynamic fragility parameter (m) of polylactides

PLLA	PLLA_m_{min}	PLLA_m_{max}	PDLLA	PDLLA_m_{min}	PDLLA_m_{max}
$C_1 = 12.7 \pm 0.7$	$C_1(-) \times T_g/C_2(+)$	$C_1(+) \times T_g/C_2(-)$	$C_1 = 10.3 \pm 0.5$	$C_1(-) \times T_g/C_2(+)$	$C_1(+) \times T_g/C_2(-)$
$C_2 = 29.1 \pm 2.4$	130.4	173.0	$C_2 = 48.6 \pm 3.9$	61.1	79.5

m_{min} and m_{max} were calculated taking into account the deviation obtained in C_1 and C_2 when fitting the experimentally obtained a_t values of the master curves to the WLF equation.

Arrhenius behavior indicating a strong glass former. On the other corner, showing a higher deviation from linearity, indicative of dynamic fragility, are found the PLLA containing the larger crystalline and RAF (PLLA-WQA). The dynamic fragility of PLLA slowly cooled from the melt (PLLA-SC), having intermediate crystallinity and RAF (see Table 1 for values), falls in between PDLLA and PLLA-WQA. Taking the derivative of the curves at $T_g/T = 1$ dynamic fragility parameters were obtained, respectively, for PDLLA and PLLA-WQA; the results are $m = 75.5$ and $m = 128.4$, showing a good agreement with the fragility parameter values of Table 2.

It is proposed that crystallinity is acting in polymeric systems as a topologycal constraint, in a similar way as silicate layer surfaces in exfoliated nanocomposites, preventing longer range dynamics and hence allowing a smaller length-scale of cooperativity of polymer chains.

4. Conclusions

Three phases, comprising a mobile amorphous fraction (MAF), a rigid amorphous fraction (RAF) and a crystalline fraction (χ_c) were found in poly(L-lactide) (PLLA). The RAF in PLLA was established after isothermal crystallization at a temperature above T_g or by non-isothermal crystallization of samples from the melt. A single MAF was adopted for PDLLA to determine the different fractions in PLLA by a three-phase model approach.

Dynamic mechanical analysis of PLLA after thermal conditioning at a sub-T_g temperature of 50 °C revealed a relaxation of chains initially in the rigid amorphous phase that partially converts to the MAF, thus giving rise to a modification in the double T_g behavior. The lower temperature tan δ peak in PLLA was coincident with the T_g of PDLLA confirming that it is a result of segmental mobility of the bulklike non-confined polylactide chains.

Our results show that amorphous PDLLA is a stronger glass former than semicrystalline PLLA. It was proved that crystallinity and RAF not only elevate T_g but also increase the dynamic fragility of polylactide chains around the T_g. These results are novel and agree with recently reported correlations between dynamic fragility and glass transition temperature for different classes of polymeric glass formers showing an increase in m with increasing T_g.

Although impediments for segmental mobility are associated to a T_g enlargement in polymeric systems, our results show that the steepness or ease with which a polymer glass former relaxes on cooling around the T_g increases with crystalline confinement, denoting a more fragile liquid behavior. The interest of the system studied is exceptional since it is demonstrative of a smaller length-scale cooperativity for the relaxation mechanism of macromolecules in nanoconfined systems, this being applicable not only to confinement by crystalline lamellae (semicrystalline polymers), but also to other macromolecular systems for instance those containing crosslinks (thermosettings) or silicate layer surfaces (nanocomposites).

Acknowledgements

The authors are thankful for financial support from the Basque Government Department of Education, University and Research (consolidated research groups GIC07/136-IT-339-07), and from Spanish Ministerio de Ciencia y Tecnología with Project MAT 2006-13436-C02-01.

References

[1] Kramarenko VY, Ezquerra TA, Sics I, Balta-Calleja FJ, Privalko VP. J Chem Phys 2000;113:447–52.
[2] Wunderlich B. Prog Polym Sci 2003;28:383–450.
[3] Lu SX, Cebe P, Capel M. Macromolecules 1997;30:6243–50.
[4] Lu SX, Cebe P. Polymer 1996;37:4857–63.
[5] Nogales A, Ezquerra TA, Batallan F, Frick B, Lopez-Cabarcos E, Balta-Calleja FJ. Macromolecules 1999;32:2301–8.
[6] Xu H, Cebe P. Polymer 2005;46:8734–44.
[7] Laredo E, Grimau M, Muller A, Bello A, Suarez N. J Polym Sci Part B Polym Phys 1996;34:2863–79.
[8] Wang Y, Gómez-Ribelles JL, Salmerón M, Mano JF. Macromolecules 2005;38:4712–8.
[9] Cangialosi D, Alegría A, Colmenero J. Europhys Lett 2005;70:614–20.
[10] Manias E, Kuppa V, Yang DK, Zax DB. Colloids Surf A Physicochem Eng Asp 2001;187:509–21.
[11] Pak J, Pyda M, Wunderlich B. Macromolecules 2003;36:495–9.
[12] Angell CA. J Non-Cryst Solids 1991;131:13–31.
[13] Angell CA. Science 1995;67:1924–35.
[14] Huang D, McKenna GB. J Chem Phys 2001;114:5621–30.
[15] Bohmer R, Ngai KL, Angell CA, Plazek J. J Chem Phys 1993;99:4201–9.
[16] Hodge IM. J Non-Cryst Solids 1996;202:164–72.
[17] Qin Q, McKenna B. J Non-Cryst Solids 2006;352:2977–85.
[18] Arnoult M, Dargent E, Mano JF. Polymer 2007;48:1012–9.
[19] Plazek DJ, Ngai KL. Macromolecules 1991;24:1222–4;
Roland CM, Ngai KL. Macromolecules 1991;24:5315–9;
Ngai KL, Plazek DJ. Macromolecules 1990;23:4282–7.
[20] Ngai KL, Roland CM. Macromolecules 1993;26:2688–90.
[21] Huo P, Cebe P. Macromolecules 1992;25:902–9.
[22] Huo P, Cebe P. J Polym Sci Part B Polym Phys 1992;30:239–50.
[23] Mijovic J, Sy JW, Kwei TK. Macromolecules 1997;30:3042–50.
[24] Sy JW, Mijovic J. Macromolecules 2000;33:933–46.
[25] Mijovic J, Sy JW. Macromolecules 2002;35:6370–6.
[26] Kanchanasopa M, Runt J. Macromolecules 2004;37:863–71.
[27] Ren J, Urakawa O, Adachi K. Macromolecules 2003;36:210–9.
[28] Bras AR, Viciosa AT, Wang Y, Dionísio M, Mano J. Macromolecules 2006;39:6513–20.
[29] Fitz BD, Jamiolkowski DD, Andjelic S. Macromolecules 2002;35:5869–72.
[30] Alves NM, Mano JF, Gómez-Ribelles JL. Polymer 2002;43:3627–33.
[31] Schindler A, Harper DH. J Polym Sci Polym Chem Ed 1979;17:2593.
[32] Zhang SH, Jing X, Painter PC, Runt J. Polymer 2004;45:3933–42.
[33] Pyda M, Bopp RC, Wunderlich B. J Chem Thermodyn 2004;36:731–42.
[34] Ohtani Y, Okumura K, Kawaguchi A. J Macromol Sci Phys 2003;B42:875–88.
[35] Pyda M, Wunderlich B. Macromolecules 2005;38:10472–9.
[36] Fischer EW, Stertzel HJ, Wegner G. Kolloid-Z.Z. Polym 1973;251:980–90.
[37] Cho TY, Strobl G. Polymer 2006;47:1036–43.
[38] Sarasua JR, Prud'homme RE, Wisniewski M, Le Borgne A, Spassky N. Macromolecules 1998;31:3895–995.
[39] Dlubek G, Sen Gupta A, Pionteck J, Häβler R, Krause-Rehberg R, Kaspar H, et al. Polymer 2005;46:6075–89.
[40] Vogel HJ. Physik Z 1921;22:645;
Fulcher GS. J Am Ceram Soc 1925;8:339;
Tammann G, Hesse WZ. Anorg Allgem Chem 1926;156:245.
[41] Williams ML, Landel RF, Ferry JD. J Am Chem Soc 1955;77:3701–7.
[42] Meaurio E, López-Rodríguez N, Sarasua JR. Macromolecules 2006;39:9291–301.